DFT and HF studies on the geometry, electronic structure and vibrational spectra of 2-nitro-tetraphenylporphyrin and zinc-2-nitro-tetraphenylporphyrin

ARTICLE *in* THE JOURNAL OF PHYSICAL CHEMISTRY A · JANUARY 2004

Impact Factor: 2.69

7 AUTHORS, INCLUDING:

Wolfgang Kiefer

University of Wuerzburg

878 PUBLICATIONS **9,837** CITATIONS

DFT and HF Studies of the Geometry, Electronic Structure, and Vibrational Spectra of 2-Nitrotetraphenylporphyrin and Zinc 2-Nitrotetraphenylporphyrin

Wei Li,[†] Yi-Bo Wang,[‡] Ioanna Pavel,[§] Yong Ye,[†] Zhang-Ping Chen,[†] Ming-Dao Luo,[†] Ji-Ming Hu,*[,†] and Wolfgang Kiefer[§]

College of Chemistry and Molecular Sciences, Wuhan University,Wuhan 430072, P.R. of China, Department of Chemistry, Guizhou University, Guiyang, Guizhou 550025, P. R. of China, and Institut für Physikalische Chemie, Universität Würzburg, Am Hubland, D-97074 Würzburg, Germany

Received: February 5, 2004; In Final Form: April 25, 2004

The ground-state geometries and electronic structures of 2-nitrotetraphenylporphyrin (H_2-2-NO_2-TPP) and zinc 2-nitrotetraphenylporphyrin (Zn-2-NO_2-TPP) with C_s and C_1 symmetry have been determined from density functional theory, using the Becke−Lee−Yang−Parr composite exchange-correlation functional (B3-LYP) and ab initio RHF method and 6-31G(d) basis set. The optimized geometries are then compared with the crystallographic data of related compounds. The energy and electronic structures of different conformers are analyzed and compared with each other. The conformers with C_1 symmetry are found to be more stable than that of C_s symmetry. The relative order of the highest occupied a_{2u} and a_{1u} orbitals determined by B3LYP ($a_{2u} > a_{1u}$) is reversed by RHF ($a_{1u} > a_{2u}$). The vibrational wavenumber, IR, and Raman intensities are also calculated at B3LYP/6-31G(d) optimized geometries. The calculated wavenumbers are scaled by a uniform scaling factor and compared with the experimental one. Most of the scaled modes are found to be in good agreement with the observed fundamentals. A single β-NO_2 substitution slightly changes the geometries, the vibrational wavenumbers, and the frontier orbitals energy level.

1. Introduction

Porphyrins and metalloporphyrins play an important role in photosynthesis, biological redox reactions, and oxygen transport and have been intensively studied for many years. The free base porphine (FBP) is the starting point for vibrational studies on metalloporphyrins, which constitute a template for very important biological functions. A resonance structure with D_{2h} symmetry has been shown to stand for FBP leading to an electronic delocalized structure for the ground state. The infrared,[1] polarized Raman,[2] and resonance Raman[3] investigations of FBP have been performed on the basis of a force field derived from scaled quantum mechanical studies (SQM). Because of the inner-hydrogen migration in FBP, the symmetry of FBP is changed among C_s, C_{2v}, and D_{2h}.[4,5]

Is the introduction of a central metal atom a perturbation sufficient to restore the symmetry to porphyrin framework? The stereochemistry of metalloporphyrins is largely determined by the relation of the unconstrained metal−nitrogen (M−N) bond length to the porphyrin cavity radius.[6] If the ideal M−N distance is significantly shorter than the cavity size, the porphyrin skeleton undergoes ruffling, i.e., a D_{2d} deformation consisting of alternate rotations of the pyrrole rings, diminishing the actual M−N distance. On the other hand, if the metal atom is too large to fit in the cavity, it is assumed that the strain is relieved by a doming distortion; i.e., the metal moves out of the porphyrin plane. Jarzecki et al.[7] and Piqueras and Rohlfing[8] have studied the electronic structures and harmonic vibrational frequencies of zinc, magnesium, and nickel porphyrins. The optimized geometries of these complexes are found to be planar and with D_{4h} symmetry. At the same time, the geometry, the charge distributions, the effect of additional charge, and ionization potentials have been also investigated by ab initio methods.[9,10]

The nature of the substituents attached to the porphyrin perimeter can determine a change in the geometry and electronic properties of the complex. More specifically, the nonplanarity of the porphyrin framework is induced by steric interactions between the bulky substituents. Because of the high symmetry, the vibrational spectra, geometries, electronic structures, and spin density profiles of tetraphenylporphyrin (TPP) and its metal complexes have been also intensively studied.[11−13] The substituent effects upon the relative energies of two highest occupied, nearly degenerate a_{2u} and a_{1u} orbitals of TPP and metallo-TPP have also been investigated by different approaches.[14−17]

In a previous study we recorded the IR and Raman spectra of 2-nitrotetraphenylporphyrin (H_2-2-NO_2-TPP) and metallo-2-nitrotetraphenylporphyrin and discussed the effect of a single β-NO_2 substitution on the mentioned spectra.[18] However, it is exceedingly difficult to develop accurate force fields for molecules of the size and complexity of H_2-2-NO_2-TPP and metallo-2-NO_2-TPP on a purely empirical basis. Quantum mechanical calculations of force constants can solve the difficulties of empirical force field determination by making independent information available, which is largely complementary to the spectroscopic measurements.[19] As an economical way of including electron correlation in the ground-state wave function, gradient-corrected density functional theory (DFT) calculations are about as expensive as the Hartree−Fock theory calculations and are much more accurate for molecules composed of first-row atoms. Wong[20] has shown that the Becke−Lee−Yang's three parameters hybrid functional (B3LYP) yield remarkably accurate vibrational wavenumbers. For the organic

* Corresponding author. E-mail: jmhu@whu.edu.cn.
[†] Wuhan University.
[‡] Guizhou University.
[§] Universität Würzburg.

10.1021/jp049477d CCC: $27.50
Published on Web 06/18/2004

molecules of the size of H_2-2-NO_2-TPP and Zn-2-NO_2-TPP, the 6-31G(d) basis set appears to be a reasonable compromise between cost and accuracy.

In this paper, the ground-state geometrical and electronic structures of H_2-2-NO_2-TPP and Zn-2-NO_2-TPP under C_1 and C_s symmetry restrictions are theoretically determined by ab initio (RHF/6-31G(d)) and DFT (B3LYP/6-31G(d)) methods. The IR and Raman spectra are then calculated at B3LYP/6-31G(d) level of theory at optimized geometries. The calculated structures are in good agreement with the available experiment values of related compounds. The molecular orbitals are analyzed and compared to each other. The influence of β-NO_2 substitution on the frontier orbitals energy is also discussed. The calibrated wavenumbers are in good agreement with the observed fundamentals.

2. Experimental and Computational Methods

H_2-2-NO_2-TPP and Zn-2-NO_2-TPP were prepared according to the literature[21] and confirmed by their elemental analysis, NMR, and mass spectra. Their FT-Raman spectra were recorded in the solid state with an IFS 120HR spectrometer equipped with an integrated FRA 106 (Brucker) Raman module. The 1064 nm radiation from a Nd:YAG laser with an output of about 150 mW was used for excitation. The spectral region of interest for the Raman spectra was 3600−150 cm^{-1}.

The ab initio calculations were performed using the restricted Hartree−Fock method. The initial search for stationary structures was carried out with the 3-21G(d) basis set under C_s and C_1 symmetry restrictions. The obtained structures were then used for the final optimization with the 6-31G(d) basis set.

Becke's 1988 exchange functional in combination with Becke's three-parameter hybrid exchange functional using the LYP correlational functional of Lee, Yang, and Parr (B3LYP) were employed in the DFT calculations. The 6-31G(d) Pople split valence basis set was chosen in the geometry optimization with C_s and C_1 symmetry and normal modes calculations of the compounds **1** and **2**. The analytically calculated vibrational wavenumbers were then scaled by 0.9614. [22]

All calculations were performed with the Gaussian 98 program [23] on an Alpha 21164/433 au workstation of GHPCC of Guizhou University.

The theoretical spectrum was simulated with the GaussSum 4.0 program. The line shape was of Lorentzian curves type and the fwhm (The full width at half-maximum of each peak) was 5 cm^{-1}. The spectral range was 150−1700 cm^{-1}.

3. Results and Discussion

3.1. Geometry. The structures of H_2-2-NO_2-TPP and Zn-2-NO_2-TPP are shown in Figure 1. Table 1 lists the selected optimized geometrical parameters of H_2-2-NO_2-TPP and Zn-2-NO_2-TPP with C_s and C_1 symmetry. For comparison purpose, the X-ray diffraction data for the toluene solvate of zinc(II) tetraphenylporphyrin (ZnTPP)[24] and triclinic tetraphenylporphyrin ($TPPH_2$)[25] are also included.

The geometrical parameters obtained from RHF/6-31G(d) calculations are in agreement with the experimental data to a degree, which is typical for this level of theory applied to large conjugated system. As expected, there are some differences in bond lengths of N−C and C−C bonds on the porphyrin ring. The calculated bond lengths of $N_1-C_{\alpha 2}$ in H_2-2-NO_2-TPP and $N_2-C_{\alpha 4}$ in Zn-2-NO_2-TPP are 0.07 and 0.05 Å shorter than the X-ray values from refs 24 and 25, respectively. The calculated $C_{\alpha 2}-C_{m1}$ distance is 0.05 Å longer than the X-ray experiment value. Other bond lengths agree within 0.03 Å. This

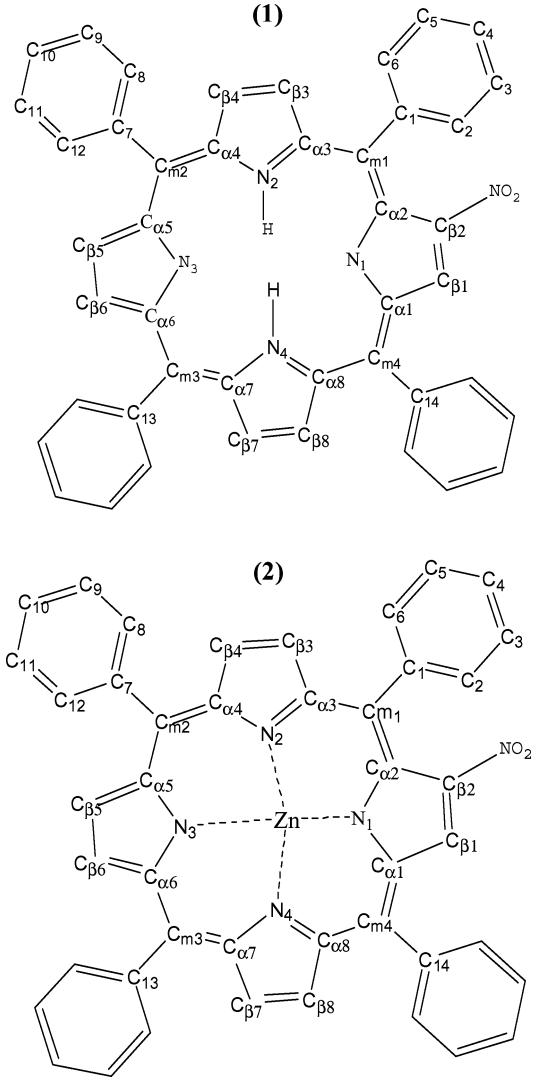

Figure 1. Atom numbering and structures of H_2−2-NO_2−TPP (**1**) and Zn−2-NO_2−TPP (**2**).

is not unexpected, since the main deficiency of RHF is the neglect of correlation effects. On the other hand, the single β-NO_2 substitution slightly changes the initial structural parameters.

The correlation effects introduced by the B3LYP/6-31G(d) level of theory correct the RHF deficiency by increasing the distances of $N_1-C_{\alpha 2}$ in H_2-2-NO_2-TPP and $N_2-C_{\alpha 4}$ in Zn-2-NO_2-TPP, respectively, and by decreasing the $C_{\alpha 2}-C_{m1}$ bond lengths. Accordingly, the $N_2-C_{\alpha 3}-C_{m1}$ and $N_2-C_{\alpha 4}-C_{m2}$ angles become smaller when correlation is included. Comparing the predicted bond lengths and bond angles of Zn-2-NO_2-TPP obtained from B3LYP/6-31G(d) calculations with the X-ray diffraction results of zinc(II) tetraphenylporphyrin (ZnTPP), one can notice that the $C_{\alpha 1}-C_{\beta 1}$ bonds are shortened by 0.015 Å, while the $C_{\alpha 1}-C_{m4}$ bonds slightly increase by 0.013 Å, due to the substitution of a single β-NO_2. The corresponding bond angles present similar variations. There are no significant effects on the other structural parameters.

Analogously, the comparison of the B3LYP/6-31G(d) predicted geometrical parameters of H_2-2-NO_2-TPP with the structure of tetraphenylporphyrin ($TPPH_2$), obtained from X-ray experiment, indicates some differences in the bond lengths and bond angles of the mentioned compounds. More exactly, they are in the range 0−0.010 Å and 0.8−1.8°, respectively. In a previous study, Jarzecki et al.[7] estimated the size of the

TABLE 1: Selected Bond Lengths, Bond Angles, and Dihedral Angles of H_2-2-NO_2-TPP and Zn-2-NO_2-TPP

	B3LYP/6-3(d)				RHF/6-31G(d)					
	H_2-2-NO_2-TPP		Zn-2-NO_2-TPP		H_2-2-NO_2-TPP		Zn-2-NO_2-TPP			
	(C_1)	(C_s)	(C_1)	(C_s)	(C_1)	(C_s)	(C_1)	(C_s)	ZnTPP[24]	$TPPH_2$[25]
					Bond Lengths (Å)					
$H-N_1$	1.014	1.014			0.996	0.994				0.93
$Zn-N_1$			2.060	2.063			2.060	2.064		
$Zn-N_2$			2.030	2.030			2.040	2.040	2.032(2)	
$Zn-N_3$			2.040	2.045			2.035	2.030	2.040(2)	
$Zn-N_4$			2.033	2.034			2.035	2.040		
$N_1-C_{\alpha1}$	1.360	1.364	1.370	1.375	1.387	1.384	1.360	1.355	1.370(2)	1.370
$N_1-C_{\alpha2}$	1.360	1.366	1.370	1.379	1.303	1.305	1.340	1.355	1.376(2)	1.359
$N_2-C_{\alpha3}$	1.370	1.376	1.370	1.378	1.378	1.372	1.390	1.380	1.373(2)	1.378
$N_2-C_{\alpha4}$	1.370	1.376	1.380	1.377	1.365	1.369	1.320	1.320	1.380(2)	1.371
$C_{\alpha1}-C_{\beta1}$	1.440	1.452	1.430	1.437	1.440	1.448	1.390	1.400	1.445(3)	1.456
$C_{\alpha1}-C_{m4}$	1.416	1.412	1.410	1.407	1.369	1.364	1.430	1.430	1.394(3)	1.400
$C_{\alpha2}-C_{\beta2}$	1.460	1.466	1.449	1.449	1.465	1.469	1.410	1.410	1.442(3)	1.455
$C_{\alpha2}-C_{m1}$	1.420	1.411	1.410	1.407	1.460	1.450	1.450	1.440	1.397(3)	1.399
$C_{\alpha3}-C_{\beta3}$	1.430	1.436	1.440	1.447	1.466	1.465	1.450	1.450	1.439(3)	1.424
$C_{\alpha3}-C_{m1}$	1.400	1.404	1.400	1.406	1.352	1.357	1.360	1.360	1.400(2)	1.397
$C_{\alpha4}-C_{\beta4}$	1.430	1.435	1.440	1.445	1.464	1.463	1.450	1.450	1.447(3)	1.432
$C_{\alpha4}-C_{m2}$	1.400	1.403	1.400	1.405	1.359	1.357	1.420	1.420	1.403(3)	1.403
$C_{\beta1}-C_{\beta2}$	1.350	1.351	1.360	1.358	1.338	1.329	1.370	1.360	1.347(3)	1.347
$C_{\beta3}-C_{\beta4}$	1.360	1.368	1.350	1.360	1.329	1.330	1.330	1.330	1.354(3)	1.355
$C_{m2}-C_7$	1.498	1.503	1.495	1.502	1.504	1.505	1.500	1.500	1.500(3)	1.502
$C_{m1}-C_1$	1.498	1.503	1.495	1.503	1.502	1.506	1.500	1.500	1.499(3)	1.506
N−O	1.233	1.229	1.230	1.228	1.193	1.192	1.190	1.190		
C−N	1.449	1.229	1.450	1.462	1.437	1.453	1.430	1.450		
					Bond Angles (deg)					
N_1-Zn-N_2			89.7	89.6			89.6	90.1	90.3(1)	
$Zn-N_1-C_{a1}$			125.3	125.4			124.1	125.0	126.9(1)	
$Zn-N_2-C_{\alpha3}$			126.4	126.9			125.1	125.5	126.3(1)	
$Zn-N_1-C_{\alpha2}$			126.1	127.0			125.8	126.4	126.4(1)	
$Zn-N_2-C_{\alpha4}$			125.6	126.6			126.2	126.3	126.8(1)	
$C_{\alpha1}-N_1-C_{\alpha2}$	106.8	106.8	107.8	107.6	107.8	107.9	108.1	108.2	106.6(1)	106.2
$C_{\alpha3}-N_2-C_{\alpha4}$	110.8	110.7	106.5	106.4	111.7	111.7	107.7	108.0	106.4(1)	109.2
$N_1-C_{\alpha1}-C_{\beta1}$	111.0	111.1	109.6	110.0	109.5	109.2	109.9	109.7	109.4(2)	110.2
$N_1-C_{\alpha2}-C_{m1}$	125.1	125.5	124.7	125.4	125.0	125.3	124.1	124.7	125.7(2)	125.8
$N_1-C_{\alpha2}-C_{\beta2}$	108.8	108.7	107.3	107.6	109.3	109.0	107.8	107.5	109.4(2)	110.3
$N_2-C_{\alpha3}-C_{m1}$	127.0	127.5	126.2	126.6	128.5	129.2	126.9	127.5	125.6(2)	126.3
$N_2-C_{\alpha4}-C_{m2}$	126.9	126.9	126.1	126.1	128.5	128.7	126.7	126.7	125.7(2)	125.7
$N_2-C_{\alpha3}-C_{\beta3}$	106.2	106.4	109.5	109.7	105.1	105.3	107.8	107.7	109.7(2)	107.3
$N_2-C_{\alpha4}-C_{\beta4}$	106.5	106.6	109.7	109.8	105.7	105.8	110.2	109.8	109.7(2)	107.3
$C_{m2}-C_{\alpha5}-C_{\beta5}$	122.2	122.9	123.8	124.5	121.9	122.1	123.8	124.0	124.8(2)	123.0
$C_{m2}-C_{\alpha4}-C_{\beta4}$	126.5	126.5	124.1	124.1	125.8	125.5	123.1	123.3	124.6(2)	126.8
$C_{m1}-C_{\alpha2}-C_{\beta2}$	125.8	125.8	127.6	127.0	125.5	125.4	127.7	127.7	124.8(2)	124.0
$C_{m1}-C_{\alpha3}-C_{\beta3}$	126.7	126.1	124.3	123.7	126.4	125.4	125.3	124.8	124.7(2)	126.5
$C_{\alpha1}-C_{\beta1}-C_{\beta2}$	105.5	105.4	106.2	106.0	105.4	105.6	105.6	105.7	107.3(2)	106.3
$C_{\alpha2}-C_{\beta2}-C_{\beta1}$	107.8	108.1	108.5	108.9	108.0	108.1	108.5	108.8	107.2(2)	107.2
$C_{\alpha3}-C_{\beta3}-C_{\beta4}$	108.3	108.2	107.1	107.1	108.8	108.8	107.5	107.5	107.3(2)	108.2
$C_{\alpha4}-C_{\beta4}-C_{\beta3}$	108.2	108.1	107.0	107.0	108.6	108.5	106.9	106.9	107.0(2)	108.0
$C_{\alpha2}-C_{m1}-C_{\alpha3}$	124.2	124.7	123.9	124.4	123.0	123.7	124.4	125.4	125.2(2)	125.6
$C_{\alpha2}-C_{m1}-C_1$	119.0	120.3	118.6	119.5	118.3	119.9	117.8	118.3	117.5(2)	117.9
$C_{\alpha3}-C_{m1}-C_1$	116.6	115.1	117.4	116.1	118.5	116.7	117.7	116.3	117.2(2)	116.5
$C_{\alpha4}-C_{m2}-C_7$	116.3	116.3	117.7	117.6	118.2	118.2	117.6	117.5	117.3(2)	116.3
$C_{\alpha8}-C_{m4}-C_{\alpha1}$	125.1	125.9	124.4	125.0	126.3	127.2	125.9	126.2	124.9(2)	125.6
$C_{\alpha1}-C_{m4}-C_{14}$	118.5	117.8	117.9	117.4	118.0	117.9	116.1	117.9	117.8(2)	116.3
					Dihedral Angles (deg)					
$C_{\alpha2}-C_{m1}-C_1-C_2$	−60.2	−91.3	−59.9	−91.3	−61.5	−91.3	−62.6	−91.3	−61.0	
$O-N-C_{\beta2}-C_{\alpha2}$	−35.7	−91.3	−38.5	−91.6	−34.9	−91.7	−36.2	−92.0		
$N_1-N_2-N_3-N_4$	−1.0	0.0	−0.4	0.0	−0.3	0.0	0.0	0.0		
$N_1-C_{\alpha2}-C_{m1}-C_{\alpha3}$	−15.7	0.0	−13.5	0.0	−21.0	0.0	−17.5	0.0		
$N_2-C_{\alpha4}-C_{m2}-C_{\alpha5}$	6.6	0.0	6.4	0.0	5.0	0.0	7.0	0.0	6.6	
$N_3-C_{\alpha6}-C_{m3}-C_{\alpha7}$	−2.5	0.0	−4.1	0.0	−3.0	0.0	−1.4	0.0	1.4	
$N_4-C_{\alpha8}-C_{m4}-C_{\alpha1}$	8.5	0.0	3.6	0.0	7.5	0.0	2.5	0.0		
$C_{\alpha4}-C_{m2}-C_7-C_8$	66.0	90.0	64.8	90.0	81.4	90.2	80.2	90.0	63.1	
total energy (au)	−2118.239	−2118.234	−3896.272	−3896.268	−2104.887	−2104.884	−3881.345	−3881.342		
dipole moment (D)	5.956	4.972	6.029	4.919	5.967	5.458	7.306	6.723		

porphyrin ring cavity, which is about 2.05 Å. If the unconstrained N−M bond is within about 0.05 Å of the cavity radius, the metal can fit without significantly altering the stereochemistry of the core. The calculated Zn−N average distance, 2.041 Å, is 0.005 Å longer than the average X-ray value of zinc(II) tetraphenylporphyrin (ZnTPP), 2.036 Å, showing that Zn-2-NO_2-TPP is nearly stress-free. The geometries optimized with C_1 symmetry are essentially the same as the ones with C_s symmetry. The bond lengths and bond angles agree within 0.01 Å and 1.5°, with the exception of the dihedral angles between the porphyrin ring plane, the four phenyl rings and a nitro group. The B3LYP/6-31G(d) and RHF/6-31G(d) calculations suggest that C_1 conformers of H_2-2-NO_2-TPP and Zn-2-NO_2-TPP are more stable than the C_s conformers (with 13.73, 10.5 kJ/mol and 7.95, 7.95 kJ/mol, respectively).

The X-ray diffraction results revealed that the atoms of the porphyrin ring are almost coplanar. However, the geometries of H_2-2-NO_2-TPP and Zn-2-NO_2-TPP optimized with C_1 sym-

TABLE 2: Orbital Energies (in eV) of H_2-2-NO_2-TPP and Zn-2-NO_2-TPP

	B3LYP/6-31G(d)					RHF/6-31G(d)						
	H_2-2-NO_2-TPP			Zn-2-NO_2-TPP		H_2−2-NO2-TPP			Zn-2-NO_2-TPP		ZNP[27]	
		(C_s)	(C_1)		(C_s)	(C_1)		(C_s)	(C_1)		(C_s)	(C_1)		$D4_h$
						Occupied (eV)								
HOMO-4	A″(π)	−6.65	−6.64	A″(π)	−6.67	−6.62	A′(σ, π)	−9.17	−9.14	A′(π)	−9.18	−9.14	e_g (π)	−6.59
HOMO-3	A″(π)	−6.57	−6.56	A″(σ)	−6.60	−6.54	A′(π)	−8.97	−8.95	A′(σ, π)	−8.92	−8.96	b_{2u}(π)	−6.58
HOMO-2	A″(π)	−6.45	−6.49	A′(σ,$d_{x^2}-d_{y^2}$)	−6.55	−6.53	A″(σ, π)	−8.89	−8.83	A″(σ, π)	−8.83	−8.81	b_{1g}(σ,$d_{x^2}-d_{y^2}$)	−6.29
HOMO-1	1a″(π)	−5.48	−5.54	1a″(π)[a]	−5.41	−5.43	2a″(π)	−7.00	−6.91	2a″(π)	−6.84	−6.87	a_{2u}(π)	−5.21
HOMO	2a″ (π)	−5.23	−5.14	2a″(π)	−5.31	−5.17	1a″(π)	−6.72	−6.81	1a″(π)	−6.42	−6.62	a_{1u}(π)	−5.21
						Unoccupied (eV)								
LUMO	A″ (π)	−2.50	−2.66	A″(π)	−2.42	−2.57	A″(π)	0.56	0.42	A″(π)	0.30	0.34	e_g(π)	−2.14
LUMO+1	A″(π)	−2.42	−2.45	A″(π)	−2.34	−2.36	A″(π)	0.69	0.75	A″(π)	0.61	0.73	e_g(π)	−2.14
LUMO+2	A′(π)	−1.63	−1.53	A′(π, s−p_z)	−1.70	−1.45	A″(π)	3.10	2.67	A″(π)	3.15	2.83	b_{1u}(π)	−0.54
LUMO+3	A″(π)	−0.85	−0.82	A″(π)	−0.79	−0.75	A′(π)	3.26	3.49	A″(π)	3.37	3.29	a_{2u}(π)	0.90
LUMO+4	A′ (σ)	−0.25	−0.29	A′(σ)	−0.26	−0.38	A′(σ)	3.63	3.61	A′(σ)	3.41	3.60	a_{1g}(σ)	1.23

[a] 1a″ and 2a″ replace a_{1u} and a_{2u}, respectively.

TABLE 3: Observed Fundamentals and Scaled Wavenumbers for H_2-2-NO_2-TPP, Together with Their IR and Raman Intensities[a]

	peak,[b]	calcd intens		obsd intens			2-NO_2-			peak,[b]	calcd intens		obsd			2-NO_2-	
mode	cm^{-1}	IR[c]	Raman	IR[18]	Raman	assign	TPP[15]	TPP[15]	mode	cm^{-1}	IR[c]	Raman	IR[18]	Raman	assign	TPP[15]	TPP[15]
12	3088	29.6	453.9		3017	υ_s(C−H)$_{Ph}$			107	986	14.0	20.9	999	1002	υ(C$_\alpha$−C$_\beta$)$_d$ + υ(N−C$_\alpha$)$_d$	1003	1002
13	3088	31.1	446.1	3053		υ_s(C−H)$_{Ph}$			109	979	1.8	247.6		968	υ(Ph)		
31	1594	6.0	616.9		1595	υ(C═C)$_{Ph}$	1598	1598	114	968	21.9	3.8	964		def of P^i		
32	1594	8.2	290.2	1595		υ(C═C)$_{Ph}$			120	949	53.2	11.8	921		υ(pyrrole)		
38	1567	114.6	230.5	1576		υ_{as}(NO_2)			129	897	5.8	1.8	883	902	γ(C−H)$_{Ph}$ + γ(C$_\beta$−H)$_p$		
39	1550	49.3	496.3		1575	υ(C$_\alpha$−C$_m$)$_P$ + υ(C$_\beta$−C$_\beta$)$_d$		1560	133	866	1.8	7.2		849	def of P^i		
40	1542	85.8	1252.0	1555	1549	υ(C$_\beta$-C$_\beta$)$_d$ + υ(C$_\alpha$−C$_m$)$_P$	1551	1554	134	860	7.1	5.3	849		def of P^i		
41	1531	24.6	678.7	1524	1518	υ(C$_\alpha$−C$_m$)$_p$	1499	1513	139	830	0.2	54.3		830	γ(C−H)$_{Ph}$		
44	1505	4.3	259.5		1492	υ(C$_\beta$−C$_\beta$)$_{p,d}$ + υ(C$_\alpha$-C$_m$)$_{P,d}$	1491	1506	145	791	114.9	0.6	798		γ(C$_\beta$-H)$_P$		
45	1497	37.3	142.8	1489		υ(C$_\beta$−C$_\beta$)$_{p,d}$ + υ(C$_\alpha$−C$_m$)$_{P,d}$			152	736	26.3	1.5	745		γ(C−H)$_{Ph}$ + γ(C$_\beta$-NO$_2$)		
51	1461	95.9	36.3	1470		υ(C$_\alpha$−C$_m$)$_d$ + υ(C$_\beta$−C$_\beta$)$_d$			154	720	66.0	5.9	721		γ(N−H)		
52	1440	25.8	298.3		1457	υ(C$_\alpha$−C$_m$)$_d$ + υ(C$_\beta$−C$_\beta$)$_d$	1459	1459	160	688	20.5	2.6	698		γ(C−H)$_{Ph}$		
57	1425	14.0	185.3	1440	1440	δ(C−H)$_{Ph}$ + υ(C$_\alpha$−C$_m$)$_{d,p}$	1440	1442	163	668	1.5	43.7	664		P, tw$_{p,d}^o$ + P, ev$_{p,d}^o$		
58	1384	28.7	16.0	1399					165	658	3.1	48.6		647	P, tw$_{p,d}^o$ +υ_{ske} of Ph		
59	1362	15.3	794.4		1383	υ(C$_\alpha$−C$_\beta$)$_d$ + δ(C$_\beta$−H)$_p$	1382	1380	168	644	14.1	1.6	656		P, ev$_p^i$+ υ_{ske} of Ph		
60	1358	283.6	509.6	1343		υ_{sym}(NO_2) + υ(C$_\alpha$−C$_\beta$)$_P$		1355	169	634	3.8	35.8	620	635	P, ev$_{p,d}^o$		
62	1341	3.4	551.8		1327	υ(N−C$_\alpha$)$_P$+υ(C$_\alpha$−C$_\beta$)$_P$			172	611	0.0	9.7		618	υ_{ske} of Ph		
69	1306	1.8	943.7	1292	1293	υ(N−C$_\alpha$)$_d$ + υ(C$_\alpha$−C$_\beta$)$_d$	1293	1296	176	577	5.8	23.6	598	566	P, tw$_p^o$		
75	1269	11.0	108.2		1273	υ(N−C$_\alpha$)$_d$+υ(C$_m$−Ph)			179	545	1.7	5.4	551		γ(Ph)		
79	1210	1.1	169.9	1233	1232	υ(C$_m$−Ph)+υ(N−C$_\alpha$)$_{d,P}$	1234	1234	182	509	8.1	2.6	510	501	γ(Ph)		
80	1208	6.6	5.6	1218	1212	δ(C$_\beta$-H)$_p$ + υ(N−C$_\alpha$)$_{d,p}$			189	403	1.8	39.1		407	γ(Ph)		
82	1189	8.1	18.5	1179	1180	δ(C$_\beta$−H)$_{p,d}$ + υ(C$_\alpha$−C$_\beta$)$_d$			192	399	0.2	23.1		367	γ(Ph)		
88	1156	102.9	37.5	1153	1157	δ(C$_\beta$−H)$_{d,P}$ + υ(N−C$_\alpha$)$_d$		1158	196	348	2.6	26.3		336	P, tr$_{p,d}^i$		
93	1115	4.1	89.5		1141	υ(N−C$_\alpha$)$_d$		1132	200	294	0.4	38.8		328	P, tr$_{p,d}^i$		
94	1090	16.7	11.6	1071		δ(C$_\beta$−H)$_{d,p}$			204	239	0.8	6.8		249	γ(C$_m$−Ph)		
95	1072	3.3	34.3		1079	δ(C$_\beta$−H)$_{d,p}$	1077	1079	211	187	0.0	31.7		201	P, βti$_{d,p}^i$		
104	1020	9.7	5.5	1029	1033	υ(C−C)$_{Ph}$	1032	1031	214	152	0.0	21.9		168	P, αti$_{p,d}^o$		

[a] Abbreviation and symbols in Table 3: υ, stretching; δ, bending; γ, wagging; tw, twist; s, symmetric; asym, asymmetric; P, pyrrole ring; Ph, phenyl; ske, skeleton; Xp and Xd, deformation X on the protonated pyrrole and deprotonated pyrrole ring, respectively; superscript "i", in-phase; superscript "o", out-of-phase; αti, tilt along the C$_\alpha$−C$_\alpha$ axis; βti, tilt along the C_2 symmetry axis; ev, envelope deformation; tr,hindered translation; ro, hindered in-plane rotation. [b] B3LYP/6-31G(d) scaling factor: 0.9614. [c] The absolute IR intensity in kM $(mol)^{-1}$ and the Raman scattering activity in $Å^4$ $(amu)^{-1}$ obtained from B3LYP/6-31G(d) calculations.

metry appear to be a slightly saddled conformer. The calculations on harmonic vibrational wavenumbers demonstrated that these conformers are stable at the local minimum point on the potential energy surface.

3.2. Ground-State Electronic Structures. The electronic spectra of porphyrin compounds are usually interpreted using the four orbital model of Gouterman,[26] which assumes that the HOMO (a_{2u}/a_{1u}) and HOMO-1 (a_{1u}/a_{2u}) of a porphyrin molecule are nearly degenerate, while the LUMO and LUMO-1 (e_g*) are rigorously degenerate. Table 2 lists the energy levels of the frontier orbitals of H2−2-NO_2-TPP and Zn-2-NO_2-TPP obtained from B3LYP/6-31G(d) and RHF/6-31G(d) calculations.

Despite being symmetry-broken, the calculation results still give a consistent picture for the frontier orbitals of these complexes. As one can notice, the energy levels of the frontier orbitals and the contribution to these orbitals calculated at different level of theories reveal some differences.

The B3LYP/6-31G(d) calculated energy differences between HOMO and HOMO-1 are 0.26, 0.10 eV and 0.39, 0.25 eV for Zn-2-NO_2-TPP and H_2-2-NO_2-TPP with C_1 and C_s symmetries, respectively. The constitutions of HOMO and HOMO-1 of Zn-2-NO_2-TPP and H_2-2-NO_2-TPP are very similar. For H_2-2-NO_2-TPP, HOMO has large contribution from the P_z orbitals of the four N atoms and the C_m atoms of the porphyrin ring. In the

TABLE 4: Observed Fundamentals and Scaled Wavenumbers for Zn-2-NO_2-TPP, Together with Their IR and Raman Intensity[a]

mode	peak,[b] cm^{-1}	calcd intens IR[c]	calcd intens Raman	obsd intens IR[18]	obsd intens Raman	assign	NiTPP[28]	ZNP[7]	mode	peak,[b] cm^{-1}	calcd intens IR[c]	calcd intens Raman	obsd IR[18]	obsd Raman	assign	NiTPP[28]	ZNP[7]
10	3088	30.0	487.1		3102	$\upsilon_s(C-H)_{Ph}$			108	983	96.0	4.9	964		υ(pyrrole)		
11	3088	30.1	383.1	3061		$\upsilon_s(C-H)_{Ph}$			109	78	0.7	290.1		971	υ(pyrrole)		
17	3077	29.7	183.7		3055	$\upsilon_{as}(C-H)_{Ph}$			120	930	2.2	6.7		909	$\gamma(C-H)_{Ph}$		
30	1595	7.8	287.1	1595		$\upsilon(C{=}C)_{Ph}$			121	907	13.2	0.4	920		$\gamma(C-H)_{Ph}$		
31	1594	4.3	604.2		1596	$\upsilon(C{=}C)_{Ph}$	1599		132	844	6.8	7.9	886	888	$\gamma(C_\beta$-H)		
36	1569	100.8	96.6	1576	1575	$\upsilon_{as}(NO_2)$			133	840	8.1	3.4	849	849	def of P^i	846	
37	1541	4.9	2334.2	1554	1548	$\upsilon(C_\beta-C_\beta) + \upsilon(C_\alpha-C_m)$	1550	(1558)	138	826	2.4	46.9		828	$\gamma(C-H)_{Ph}$		
								1544	140	810	1.8	3.4		808	def of P^i + $\gamma(C-H)_{Ph}$	828	
40	1520	51.3	153.3	1519	1516	$\upsilon(C_\beta-C_\beta) + \delta(C_\beta$-H)	1510	(1517)	141	786	60.3	1.2	795	785	$\delta(NO_2)$		
41	1499	53.1	343.5	1488	1494	$\upsilon(C_\beta-C_\beta) + \delta(C_\beta-H)$	1504	1494	148	737	37.0	4.7	753	763	$\gamma(C_\beta$-$NO_2)$		
47	1472	82.1	34.7	1460		$\upsilon(C_\alpha-C_m)$	1485		151	715	19.9	6.5	719	735	P, tw^o + P, ev^o		
49	1446	1.2	816.6		1455	$\upsilon(C_\alpha-C_m) + \delta(C_\beta-H)$			155	688	19.4	2.2	702		$\gamma(C-H)_{Ph}$	701	
50	1439	21.6	75.6	1440	1440	$\upsilon(C_\beta-C_\beta) + \upsilon(C_\alpha-C_m)$	1470	(1438)	158	675	3.7	28.8		684	P, tw^o		
								1431	160	663	4.8	38.1	661	664	υ_{ske} of Ph + P, tw^o		
57	1360	326.6	345.2	1365	1362	$\upsilon_s(NO_2)$			162	653	15.8	20.0		639	υ_{ske} of Ph	639	
58	1346	7.9	1929.0		1346	$\upsilon(N-C_\alpha) + \upsilon(C_\alpha-C_\beta) + \delta(C_\beta-H)$	1341	1347	164	648	17.9	1.4	621		υ_{ske} of Ph		
									167	611	0.3	9.3		619	υ_{ske} of Ph		
59	1338	26.1	566.1	1332	1323	$\upsilon(N-C_\alpha) + \upsilon(C_\alpha-C_\beta)$			170	583	7.6	18.3	596	597	P, tw^o		
68	1283	1.2	34.2	1291	1290	$\upsilon(N-C_\alpha) + \upsilon(C_\alpha-C_\beta)$	1302	(1299)	172	554	4.1	3.9	557		γ(Ph)		
74	1247	2.3	164.9	1272	1276	$\upsilon(N-C_\alpha)+\upsilon(C_m-Ph)$	1269		174	546	1.3	5.4		559	$\gamma(C_m-Ph)$	560	
76	1214	25.9	347.4	1229		$\upsilon(N-C_\alpha)+\upsilon(C_m-Ph)$			176	515	6.8	3.6	494		γ(Ph)		
77	1212	6.7	966.8		1235	$\upsilon(C_m-Ph)+\upsilon(N-C_\alpha)$	1235		179	481	0.1	6.7		494	γ(Ph)	498	
79	1193	10.4	18.3		1203	$\upsilon(N-C_\alpha) + \delta(C_\beta-H)$			187	401	0.14	41.9		404	γ(Ph)	390	
80	1182	26.5	16.5	1192	1192	$\delta(C_\beta-H)+ \upsilon(C_\alpha-C_\beta)$	1190		189	389	5.6	47.2		395	υ(Zn−N)	402	367
81	1168	3.2	20.0	1176	1176	$\delta(C-H)_{Ph}$			190	383	7.4	29.0		370	υ(Zn−N)		
89	1144	17.2	55.4	1152	1154	$\delta(C_\beta-H) + \upsilon(N-C_\alpha)$		(1151)	191	323	0.11	1.1		341	P, α ti^o		
90	1101	13.4	5.7	1112		$\delta(C_\beta-H)$			192	317	1.3	28.5		318	υ(Zn−N)	277	
91	1074	3.9	25.2	1070		$\delta(C_\beta-H)$	1084	(1052)	195	288	0.3	8.8		288	P, αti^o		
92	1070	3.3	59.8		1073	$\delta(C_\beta-H)$	1079	1070	197	273	0.4	3.8		278	$\gamma(C_m-Ph) + \tau(C-C)_{Ph}$		
101	1020	0.2	64.0		1030	$\upsilon(C-C)_{Ph}$	1034		199	245	0.8	7.2		249	$\gamma(C_m-Ph) + \tau(C-C)_{Ph}$	238	
102	1006	11.1	19.3	1029		$\upsilon(C-C)_{Ph}$			206	194	0.2	31.6		200	P, tr^i	202	
103	1004	2.4	91.6		1003	$\upsilon(N-C_\alpha) + \upsilon(C_\alpha-C_\beta)$	1005	997	210	163	2.4	20.5		174	P, tr^i		
104	999	6.8	23.4	1001		$\upsilon(N-C_\alpha) + \upsilon(C_\alpha-C_\beta)$		(993)									

[a] Abbreviation and symbols in Table 4: υ, stretching; δ, bending; γ, wagging; tw, twist; s, symmetric; asym, asymmetric; P, pyrrole ring; Ph, phenyl, ske; skeleton, Xp and Xd, deformation X on the protonated pyrrole and deprotonated pyrrole ring, respectively; superscript "i", in-phase; superscript "o", out-of-phase; αti, tilt along the $C_\alpha-C_\alpha$ axis; βti, tilt along the C_2 symmetry axis; ev, envelope deformation; tr, hindered translation; ro, hindered in-plane rotation. [b] B3LYP/6-31G(d) scaling factor: 0.9614. [c] The absolute IR intensity in kM $(mol)^{-1}$ and the Raman scattering activity in $Å^4$ $(amu)^{-1}$ were obtained from B3LYP/6-31G(d) calculations.

same way, the HOMO of Zn-2-NO_2-TPP has large contributions from the P_z orbitals of the four N atoms and the C_m atoms of the porphyrin ring, as well as from the P_z and d orbitals of the zinc atom. It seems that HOMO of Zn-2-NO_2-TPP is considerably stabilized by the interaction between the P_z orbitals of the N atoms and the P_z and d orbitals of the zinc atom. Under C_1 and C_s symmetry restrictions, the energy level of HOMO of Zn-2-NO_2-TPP is lowered by 0.03 and 0.08 eV, respectively, in comparison with that of H_2-2-NO_2-TPP. Both HOMO-1 orbitals mainly consist of the P_z orbitals of the C_α atoms of the porphyrin ring.

The energy levels of the frontier orbitals determined by RHF method are significantly different from those given by the B3LYP/6-31G(d) method. The energy differences between HOMO and HOMO-1 are 0.42, 0.25 eV and 0.38, 0.10 eV for Zn-2-NO_2-TPP and H_2-2-NO_2-TPP under C_s and C_1 symmetry restrictions, respectively. Moreover, the characteristic contributions to the HOMO and HOMO-1 are completely reversed. The B3LYP/6-31G(d) calculations show that HOMO of Zn-2-NO_2-TPP and H_2-2-NO_2-TPP has large contributions from the P_z orbitals of the C_α atoms of the porphyrin ring, while HOMO-1 mainly consists of the P_z orbitals of the four N atoms and the C_m atoms of the porphyrin ring. The HOMO and HOMO-1 obtained by the B3LYP/6-31G(d) have a_{2u} and a_{1u} characters, respectively. The relative order of two highest occupied orbitals is $a_{2u} > a_{1u}$, which is consistent with previous studies results.[12,17] However, the RHF calculations show that HOMO and HOMO-1 are mainly characteristic of a_{1u} and a_{2u} orbitals, respectively. The relative order of the two highest occupied orbitals is $a_{1u} > a_{2u}$.

Electron-donating groups at the pyrrole β-position raise the energy of the a_{1u} orbital, while electron-donating groups at methylene bridges raise the energy of the a_{2u} orbital. In the Zn-2-NO_2-TPP compound, the phenyl is an electron-donating group; i.e., the energy of the a_{2u} orbital increases. The nitro group is an electron-withdrawing group, which only slightly enlarges the a_{2u}/a_{1u} separation. Comparing the energy levels of HOMO of Zn-2-NO_2-TPP obtained from B3LYP/6-31G(d) calculations with that of ZnP,[27] one can notice that the energy level of Zn-2-NO_2-TPP raises by 0.04 eV.

The energy levels of LUMO and LUMO-1 are very close. They are mainly composed of the π system of the porphyrin ring. The four frontier orbitals are well separated from other levels. The B3LYP/6-31G(d) calculated energy levels of LUMO and LUMO-1 for the conformers with C_s symmetry are more rigorously degenerate than those for the conformers with C_1 symmetry.

The DFT results indicate a significantly smaller positive charge on the Zn atom than that obtained by the RHF method. The B3LYP/6-31G(d) calculated charges on the Zn and H atoms are 0.93 and 0.41 e, respectively. The N atom has a negative charge of −0.76 e. The RHF calculations reveal a higher positive

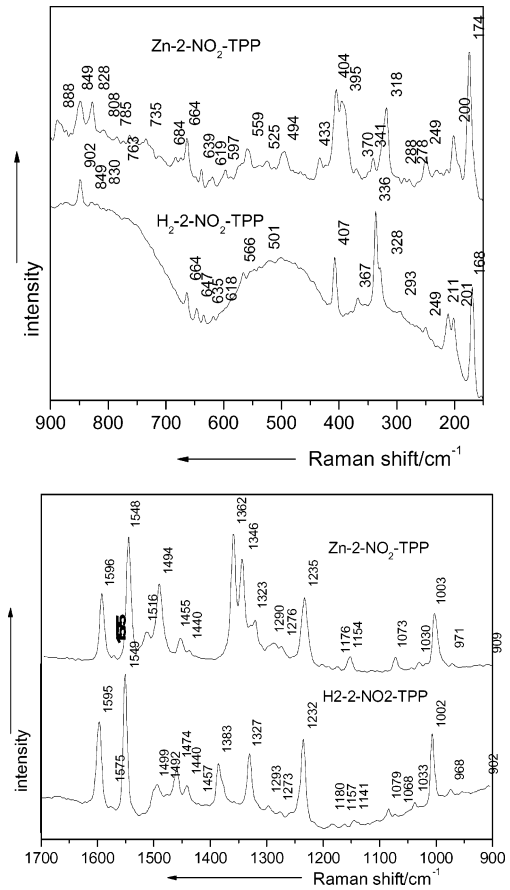

Figure 2. FT-Raman spectra of Zn−2-NO_2−TPP and H_2−2-NO_2−TPP.

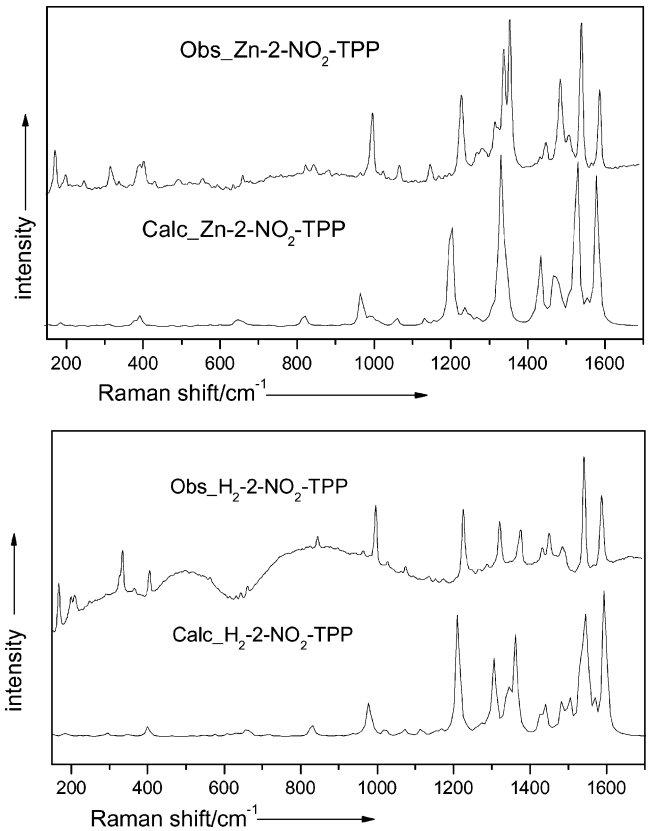

Figure 3. Comparison between the simulated theoretical and experimental spectra.

charges for the Zn and H atoms (1.32 and 0.44 e, respectively), and also an important negative charge on the N atom (−0.95 e). All these results indicate a significant charge transfer from the zinc or hydrogen atom to the porphyrin ring.

3.3. Vibrational Wavenumbers. The vibrational wavenumbers and IR and Raman intensities of H_2-2-NO_2-TPP and Zn-2-NO_2-TPP were determined by B3LYP with a 6-31G(d) basis set at optimized geometry with C_1 symmetry. It is known that ab initio and DFT potentials systematically overestimate the vibrational wavenumbers. These discrepancies can be corrected by directly scaling the calculated values with a proper factor.[22] According to the calculated wavenumbers and their intensities, the normal-mode analysis and the literature,[1−3,15,18,28] the experimental fundamentals are then assigned (Tables 3 and 4). Also, the FT-IR spectra of H_2-2-NO_2-TPP and Zn-2-NO_2-TPP, the resonance Raman spectra of NiTPP,[28] H_2-2-NO_2-TPP, and H_2TPP,[15] and the Raman spectrum of ZnP[7] are presented in Tables 3 and 4.

H_2-2-NO_2-TPP and Zn-2-NO_2-TPP with C_1 symmetry have 234 and 231 vibrational modes, respectively. The absence of imaginary wavenumbers confirms that the local minima on the potential energy surface have been found. Comparing the scaled wavenumbers with the experimental fundamentals, it can be seen that the deviations are typically less than 30 cm^{-1} (except for a few cases when it is out of the specified range).

The FT-Raman spectra of H_2-2-NO_2-TPP and Zn-2-NO_2-TPP are presented in Figure 2. For comparison purpose, the simulated spectra and experimental spectra are also listed in Figure 3 together.

From Figure 2, one can notice that the FT-Raman spectra of H_2-2-NO_2-TPP and Zn-2-NO_2-TPP reveal far-reaching similarities in most of the band patterns. Some differences appear in the position and relative intensity of some bands. The normal-mode analysis and the experimental spectra show that the characteristic skeletal vibrational modes of the parent TPP are presented in all FT-Raman spectra of H_2-2-NO_2-TPP and Zn-2-NO_2-TPP. Moreover, the incorporation of a NO_2 group in the TPP and Zn-TPP molecules does not lead to any substantial spectral changes, and on the whole FT-Raman spectra of H_2-2-NO_2-TPP, Zn-2-NO_2-TPP, and initial TPP retain their similarity.

Most of the assignments of FT-IR and FT-Raman bands are identical with findings presented in the literature, with the exception of a few peak assignments. First, as marked bands for H_2-2-NO_2-TPP, the asymmetric and symmetric stretching vibrations of the NO_2 group show up at 1576 and 1343 cm^{-1} in the FT-IR spectrum and do not appear in the FT-Raman spectra. The theoretical results indicate mode 39 to have a stronger Raman intensity than that of mode 38, so the peak at 1575 cm^{-1} can be assigned to the $C_\alpha-C_m$ stretching accompanied by the $C_\beta-C_\beta$ stretching vibration in the pyrrole ring, which is consistent with ref 28. On the contrary, for Zn-2-NO_2-TPP, all these modes are active in IR and Raman spectra. The asymmetric and symmetric stretching vibrations of NO_2 group appear at 1576 and 1365 cm^{-1} in the FT-IR spectrum and at 1575 and 1362 cm^{-1} in the FT-Raman spectrum. At the same time, the bending vibration of the NO_2 group occurs at 795 cm^{-1} in the FT-IR spectrum. Because the IR intensity of the out-of-plane deformation of $C_\beta-H$ is stronger than that of the NO_2 bending vibration, the peak at 798 cm^{-1} in the FT-IR spectrum of H_2-2-NO_2-TPP can be assigned to the $C_\beta-H$ out-of-plane deformation.

The peaks at 1524 cm^{-1} in the FT-IR and 1518 cm^{-1} in the FT-Raman spectrum of H_2-2-NO_2-TPP can be ascribed to the

stretching vibration of $C_\alpha-C_m$. However, the corresponding signals at 1519 cm^{-1} in the FT-IR spectrum and 1516 cm^{-1} in the FT-Raman spectrum of Zn-2-NO_2-TPP arise from the stretching mode of $C_\beta-C_\beta$ in combination with the bending vibration of $C_\beta-H$. In ref 28, the peak at 1504 cm^{-1} in the RR spectrum of NiTPP was attributed to the stretching motion of $C_\beta-C_\beta$ coupled with a $C_\beta-H$ bending. In ref 15, the band at 1513 cm^{-1} in the RR spectrum of H2−2-NO_2-TPP was also attributed to the stretching vibration of $C_\beta-C_\beta$.

The peaks at 1489 and 1492 cm^{-1} in the FT-IR and FT-Raman of H_2-2-NO_2-TPP, respectively, are identified as $C_\alpha-C_m$ stretching accompanied by a $C_\beta-C_\beta$ stretching vibration in the pyrrole ring. The corresponding mode was observed at 1491 and 1506 cm^{-1} in the RR spectra of TPP and H2−2-NO_2-TPP,[15] respectively. However, in the FT-IR and Raman spectrum of Zn−NO_2-TPP, the bands at 1488 and 1494 cm^{-1}, respectively, are attributed to the stretching vibration of $C_\beta-C_\beta$ in combination with a $C_\beta-H$ bending.

The insertion of Zn atom in the center of the molecule results in new vibrational modes. The stretching vibrations of Zn−N can be observed at 395 and 318 cm^{-1} in the FT-Raman spectrum of Zn-2-NO_2-TPP. The corresponding stretching vibrations of Ni−N were detected at 402 and 277 cm^{-1} in the RR spectrum of NiTPP.[28] For H_2-2-NO_2-TPP, the stretching mode of N−H does not appear in the Raman and IR spectra, but the out-of-plane deformation of N−H can be observed at 721 cm^{-1} in the FT-IR measurement. In ref 18, the peak at 1638−1653 cm^{-1} in FT-IR spectra had been attributed to the $C_\alpha-C_m$ stretching vibration, but in our calculation, there are no modes in the 3000−1600 cm^{-1} range. Therefore we consider it to be noise. The other bands assignments are essentially the same.

Comparing the FT-Raman spectrum of Zn-2-NO_2-TPP with the RR spectrum of NiTPP[28] and the Raman and IR spectra of ZnP,[7] it may be concluded that the incorporation of phenyl and nitro substitution do not significantly modify the spectral pattern. Due to the symmetry being broken, all vibrations become active in both IR and Raman spectra of Zn-2-NO_2-TPP.

4. Conclusions

The ground-state geometries of H_2-2-NO_2-TPP and Zn-2-NO_2-TPP have been optimized with DFT (B3LYP/6-31G(d)) and ab initio (RHF/6-31G(d)) methods, under C_s and C_1 symmetry restriction. The harmonic vibrational wavenumbers are determined at the geometry optimized at the B3LYP/6-31G-(d) level of theory. The calculated geometrical parameters are then compared with the available experiment values of related compounds. The conformers with C_1 symmetry are found to be more stable than that of C_s symmetry. The structures predicted by B3LYP/6-31G(d) are better than those obtained from RHF/6-31G(d). The incorporation of the nitro group does not significantly change the main framework of TPP. The energy order of the frontier orbitals is degenerated, probably due to the effect induced by peripheral substituents. Moreover, the relative order of two highest occupied a_{2u} and a_{1u} orbitals of H_2-2-NO_2-TPP and Zn-2-NO_2-TPP obtained from B3LYP/6-31G(d) calculations is a2u > a1u, which is the inverse of that obtained by RHF/6-31G(d) method. The calculated wavenumbers are calibrated with a uniform scaling factor, and they are found to be in good agreement with the experimental values.

Acknowledgment. Financial support from the Deutsche Forschungsgemeinschaft (Grants 446 CHV-112/46/01 and 446 CHV-112/52/02) and the National Natural Science Foundation of China (Grants 20375029, 20111130695, and 20211130525) is highly acknowledged. W.K. and I.P. thank the Fonds der Chemischen Industrie for financial support.

Supporting Information Available: Unabridged versions of Tables 3 and 4. This material is available free of charge via the Internet at http://pubs.acs.org.

References and Notes

(1) Kozlowski, P. M.; Jarzecki, A. A.; Pulay, P. *J. Phys. Chem.* **1996**, *100*, 7007−7013.
(2) Kozlowski, P. M.; Jarzecki, A. A.; Pulay, P. *J. Phys. Chem.* **1996**, *100*, 13985−13992.
(3) Tazi, M.; Lagant, P.; Vergoten, G. *J. Phys. Chem. A* **2000**, *104*, 618−625.
(4) Boronat, M.; Ortí, E.; Viruela, P. M.; Tomás, F. *J. Mol. Struct. (THEOCHEM)* **1997**, *390*, 149−156.
(5) Baker, J.; Kozlowski, P. M.; Jarzecki, A. A.; Pulay, P. *Theor. Chem. Acc.* **1997**, *97*, 59−66.
(6) Scheidt, W. R. In *The porphyrins*; Dolphin, D., Ed.; Academic: New York, 1978; Vol. 3, pp 463−511.
(7) Jarzecki, A. A.; Kozlowski, P. M.; Pulay, P.; Ye, B. H.; Li, X. Y. *Spectrochim. Acta A* **1997**, *53*, 1195−1209.
(8) Piqueras, M. C.; Rohlfing, C. M. *Theor. Chem. Acc.* **1997**, *97*, 81−87.
(9) Zwaans, R.; van Lenthe, J. H.; den Boer, D. H. W. *J. Mol. Struct. (THEOCHEM)* **1995**, *339*, 153−160.
(10) Zwaans, R.; van Lenthe, J. H.; den Boer, D. H. W. *J. Mol. Struct. (THEOCHEM)* **1996**, *367*, 15−24.
(11) Lu, Q. Z.; Yu, R. Q.; Shen, G. L. *J. Mol. Catal. A: Chem.* **2003**, *198*, 9−22.
(12) Lie, T. R.; Ghosh, A. *J. Am. Chem. Soc.* **2002**, *124*, 8122−8130.
(13) Ma, S. X.; Yue, Q. J.; Li, Z. *Sci. China Ser. B* **2000**, *30*, 103−109.
(14) Chirvony, V. S.; Hock, A. V.; Schaafsma, T. J.; Pershukevich, P. P.; Filatov, I. V.; Avilov, I. V.; Shishporenok, S. I.; Terekhov, S. N.; Malinovskii, V. L. *J. Phys. Chem. B* **1998**, *102*, 9714−9724.
(15) Terekhov, S. N.; Chirvonyi, V. S.; Turpin, P. Y. *J. Appl. Spectrosc.* **2000**, *67*, 796−805.
(16) Wojaczyński, J.; Crazyński, L. L.; Hrycyk, W.; Pacholska, E.; Rachlewicz, K.; Szterenberg, L. *Inorg. Chem.* **1996**, *35*, 6861−6872.
(17) Sibilia, S. A.; Czernuszewicz, R. S.; Crossley, M. J.; Spiro, T. G. *Inorg. Chem.* **1997**, *36*, 6450−6453.
(18) Hu, J. M.; Pavel, I.; Moigno, D.; Wumaier, M.; Kiefer, W.; Chen, Z. P.; Ye, Y.; Wu, Q.-F.; Huang, Q. M.; Chen, S. Q.; Niu, F.; Gu, Y. H. *Spectrochim. Acta A* **2003**, *59*, 1929−1935.
(19) Pulay, P. In *Applications of Electronic Structure Theory*; Schaefer, H. F., III, Ed.; Plenum: New York, 1977, p 153.
(20) Wong, M. W. *Chem. Phys. Lett.* **1996**, *256*, 391−399.
(21) Binstead, R. A.; Crossley, M. J.; Hush, N. S. *Inorg. Chem.* **1991**, *30*, 1259−1264.
(22) Scott, A. P.; Radom, L. R. *J. Phys. Chem.* **1996**, *100*, 16502−16513.
(23) Frisch, M. J.; Trucks, G. W.; Schlegel, H. B.; Scuseria, G. E.; Robb, M. A.; Cheeseman, J. R.; Zakrzewski, V. G.; Montgomery, J. A.; Stratmann, Jr. R. E.; Burant, J. C.; Dapprich, S.; Millam, J. M.; Daniels, A. D.; Kudin, K. N.; Strain, M. C.; Farkas, O.; Tomasi, J.; Barone, V.; Cossi, M.; Cammi, R.; Mennucci, B.; Pomelli, C.; Adamo, C.; Clifford, S.; Ochterski, J.; Petersson, G. A.; Ayala, P. Y.; Cui, Q.; Morokuma, K.; Malick, D. K.; Rabuck, A. D.; Raghavachari, K.; Foresman, J. B.; Cioslowski, J.; Ortiz, J. V.; Stefanov, B. B.; Liu, G.; Liashenko, A.; Piskorz, P.; Komaromi, I.; Gomperts, R.; Martin, R. L.; Fox, D. J.; Keith, T.; Al-Laham, M. A.; Peng, C. Y.; Nanayakkara, A.; Gonzalez, C.; Challacombe, M.; Gill, P. M. W.; Johnson, B.; Chen, W.; Wong, M. W.; Andres, J. L.; Gonzalez, C.; Head-Gordon, M.; Replogle, E. S.; Pople, J. A. *Gaussian 98*; Gaussian Inc.: Pittsburgh, PA, 1998.
(24) Scheidt, W. R.; Kastner, M. E.; Hatano, K. *Inorg. Chem.* **1978**, *17*, 706−710.
(25) Silvers, S. J.; Tulinsky, A. *J. Am. Chem. Soc.* **1967**, *89*, 3331−3337.
(26) Gouterman, M. *J. Mol. Spectrosc.* **1961**, *6*, 138−163.
(27) Chen, D. M.; Liu, X.; He, T. J.; Liu, F. C. *Chem. Phys. Lett.* **2002**, *361*, 106−114.
(28) Li, X. Y.; Czernuszewicz, R. S.; Kincaid, J. R.; Su, Y. O.; Spiro, T. G. *J. Phys. Chem.* **1990**, *94*, 31−47.